4.1 AO Control and Simulations

Jared R. Males

1 Introduction

Here we describe our end-to-end simulations of MagAO-X. The requirement for these simulations is to demonstrate that the overall MagAO-X architecture and components can control atmospheric turbulence well enough to deliver the contrast and Strehl required for MaXProtoPlanets. This includes evaluation of the options we are considering for woofer-tweeter control and showing that they are each viable.

2 Wavefront Control Strategies

We are considering several different control strategies, each with pros and cons.

2.1 Phase I: In Phase I no new high-order wavefront control will be added. The existing MagAO system, with 585 actuators running at up 2kHz, will provide the correction. A beamsplitter at the input to MagAO-X will send some fraction of the light to the MagAO PWFS, and the rest will enter MagAO-X. The vAPP coronagraph will be used, and low-order wavefront sensing and control will occur using the coronagraph channel LOWFS-DM. Figure 1 shows a block diagram of the major components of this phase.

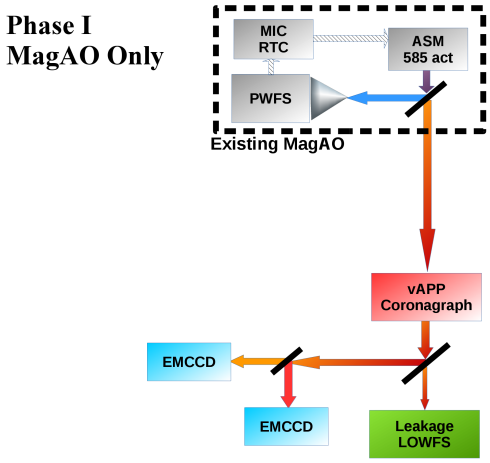

Figure 1: Phase I: all high order wavefront correction is by the existing MagAO system.

.

2.2 Phase II: In Phase II we will implement high-order wavefront control using the MEMS 2k with 2048 actuators total. Assuming a 1.5 μm stroke device is used, we will augment it with either a first stage or a woofer. There are three possible strategies:

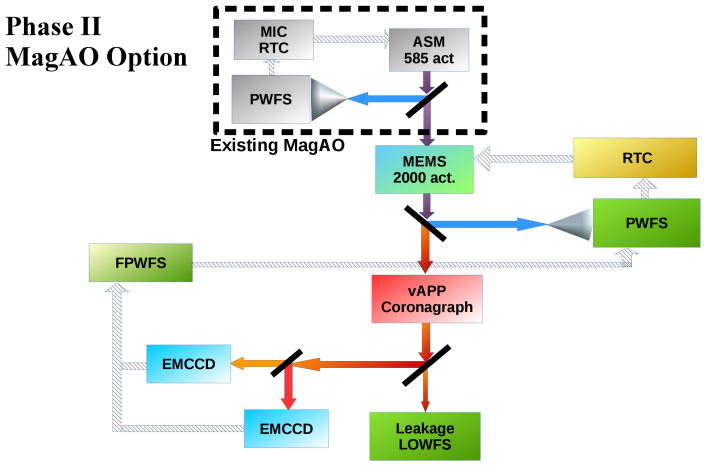

Figure 2: Phase II MagAO Option: Existing MagAO is used as an independent first stage (as is done with AO 188 at SCExAO).

.

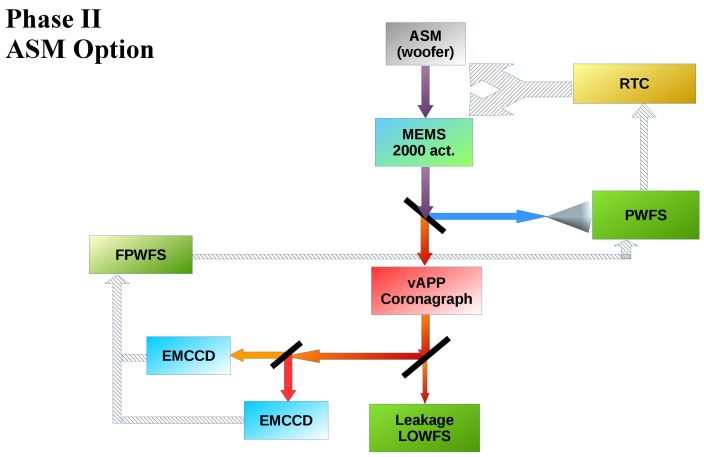

Figure 3: Phase II ASM Option: The MagAO ASM is used as a woofer, with all wavefront sensing by the MagAO-X PWFS.

.

- The existing MagAO system could be used as an independent first stage. This is what is currently done at Subaru with SCExAO and AO188. Some fraction of the incoming light would be sent to the MagAO PWFS, and the rest used in MagAO-X. The main benefit is the simplicity: only the MEMS needs to be controlled by our new system. The drawbacks are that few photons are available for MagAO-X PWFS, and the dynamics are sub-optimal in that the overshoot of existing MagAOs control will be in the temporal bandwidth of MagAO-X for low spatial-frequencies. This is shown schematically in Figure 2.
- The MagAO ASM could be used as a woofer. Here the new MagAO-X PWFS gets all the photons in the WFS band, and control is split between the ASM (low orders) and MEMS (high orders). The benefits are

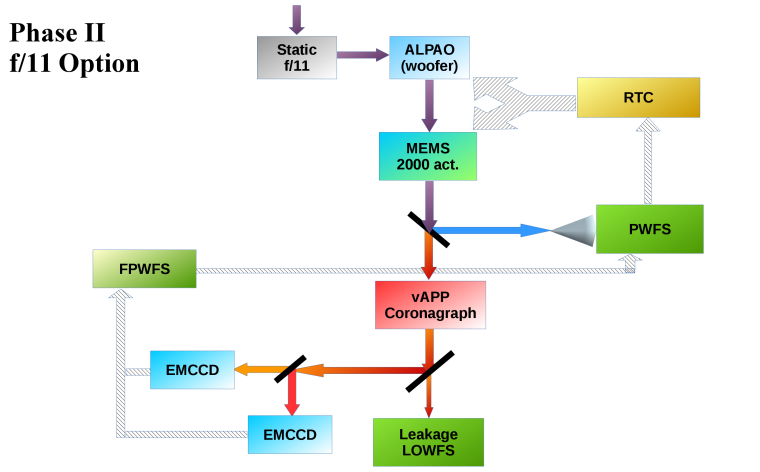

Figure 4: Phase II f/11 Option: The static f/11 secondary is used, all wavefront sensing is by the MagAO-X PWFS, and an on-board woofer is used.

.

efficient use of photons. The major drawback is that system calibration requires access to the ASM on the telescope. This is shown schematically in Figure 3.

- A further option we are considering (and the one we prefer) is to use the static f/11 secondary, and add a woofer to MagAO-X. The benefits are in the efficient use of photons for WFS, and this significantly improves the concept of operations due to being able to do nearly all AO calibrations off the telescope, and the relative ease of scheduling observing runs. The drawback is an additional 4 optics to relay onto the woofer. This is likely mitigated by the much fresher coating on the f/11 compared to the ASM, meaning we expect only a minor throughput loss. This is shown schematically in Figure 4.

- A final possibility is that BMC is successful in delivering a 3.5 μm stroke device, largely obviating the need for a woofer. Here we would use the f/11, and would likely still relay to the Alpao DM to offload the lowest orders from the MEMS (i.e. minimize stroke use to flatten) and to handle large non-Kolmogorov disturbances, e.g. from telescope vibrations.

The opto-mechanical design admits all of the above options to be used, and we have not yet committed to a single one. Our current preference is for the static f/11 with woofer option, due to the great simplification in the concept of operations. We intend to keep all of the above options open for some time as we implement the system and determine which one provides the best performance.

3 Simulations

We have conducted extensive end-to-end simulations to quantify the performance of MagAO-X and allow evaluation of the various control possibilities. Here we give details of the simulations. In the simulations all propagation is performed using the Fraunhofer approximation.

3.1 Pyramid Sensor: We simulate the pyramid using a fully diffractive model, which includes interference between the quadrants. Each quadrant has a tip OPD applied, calculated to place the subsequent pupil images in

Table 1: MagAO PyWFS Specifications

Parameter	Value	Notes
Readout Noise	3-25 e^-	depends on readout rate
Max frame rate	2000 fps	Max rate
λ_0	0.842 μm	See throughput document
$\Delta\lambda$	0.261 μm	See throughput document
Throughput	0.112	See throughput document
Modulation Radius	3.0 λ/D	
Pupil Diameter	30 pixels	can be binned

Table 2: MagAO-X PyWFS Specifications

Parameter	Value	Notes
Readout Noise	150 e^-	
EM Gain	500	
Effective RON	0.3 e^-	
Dark Current	20 $e^-/pix/sec$	Upper limit at 2000 fps
Clock Induced Charge	0	Assumed negligible
Max frame rate	3630 fps	Max stable rate at SCExAO
λ_0	0.851 μm	See throughput document
$\Delta\lambda$	0.257 μm	See throughput document
Throughput	0.227	See throughput document
Modulation Radius	0.0 - 3.0 λ/D	
Pupil Diameter	56 pixels	See lens design

the correct location. The images are binned to 120x120, such that the pupil images are 56 pixels in diameter. The binning preserves flux.

Modulation is simulated by applying tilts in the pupil plane prior to the pyramid. We use a number of discrete modulation steps so that there are at least 2 per λ/D along the circular modulation path. The MagAO pyramid is simulated using its nominal parameters, including the CCD-39. See Table 1. The MagAO-X pyramid simulation is based on the optical design and the specifications for the OCAM-2K EMCCD. See Table 2 and Figure 5.

3.2 Deformable Mirrors:

3.2.1 Tweeter: MagAO-X will use a Boston Micromachines 2k MEMS deformable mirror as the tweeter. The specifications of this device are summarized in Table 3. In the simulator we model this device using Gaussian influence functions, which are a very good match to a BMC DM. BMC specifies a coupling, which is the height of the influence function at the position of a neighboring actuators. The coupling specified is $15\pm3\%$. We generated a simulated mirror with actuators assigned an influence function with width drawn from a uniform distribution to produce coupling across this range. The pseudo-inverse of the influence function map is calculated, which is then projected on to the desired modal basis set to generate the "modes-to-commands" (M2C) matrix. This allows us to go from modal amplitudes (determined by the PyWFS and controller, described below) to a mirror command in physical units.

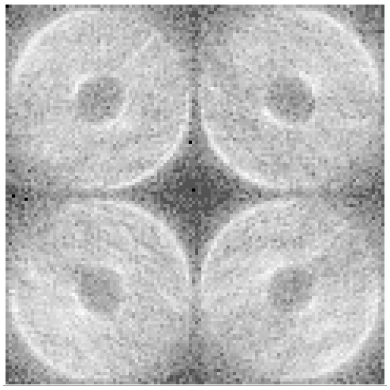

Figure 5: Simulated MagAO-X PWFS Image. This is for an 8th magnitude star, with a log stretch to illustrate the noise simulation.

Table 3: BMC 2k Tweeter Specifications

Parameter	Value	Notes
Total Actuators	2048	
Actuators Across	50	
Coupling	15%	
Settling Time	0.06 ms	
Max Frequency	∼10 kHz	
Interactutor Stroke	0.85 μm	Surface
Row-up/down Stroke	1.1 μm	Surface
4x4 Stroke	2.1 μm	Surface

Table 4: Alpao DM97-15 Woofer Specifications . These are from the test report for the as-delivered device.

Parameter	Value	Notes
Total Actuators	97	
Actuators Across	11	
Coupling	40%	
Settling Time	0.33 ms	
Max Frequency	2196 Hz	
Interactutor Stroke	2.24 μm	Surface
3x3 Stroke	4.5 μm	Surface
Tip/Tilt Stroke	15 μm	Surface, reduced for high speed
Focus Stroke	12.5 μm	Surface
Astig. Stroke	12.5 μm	Surface
Coma Stroke	9 μm	Surface

3.2.2 Woofer: When using the f/16 ASM option, the existing MagAO system serves as the woofer. To model the ASM we simply use the Karhunen Loeve modal basis measured interferometrically, that is we do not simulate

individual actuators.

For the f/11 option, we will need a woofer on the MagAO-X bench. We have chosen the Alpao DM97-15 with high speed option to serve as the woofer. We have procured a DM97 (using startup funds) to begin testing it to verify that it is suitable for this purpose. Its characteristics are summarized in table 4.

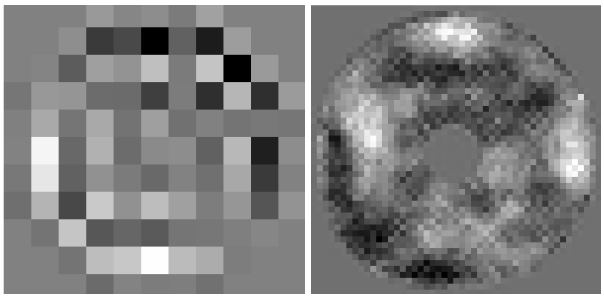

Figure 6: Actuator commands during simulation. At left for the DM97 woofer, and at right the 2k tweeter.

3.2.3 Modeling DM Stroke Limits: The BMC and Alpao mirrors have well documented stroke limits, as listed in the tables. The various limits have complicated relationships, and we do not simulate the physics of the facesheet so it is difficult to capture this. However, the inter-actuator stroke limits are the most limiting and so we enforce them in our simulations. If any two actuators reach the inter-actuator stroke limit for the device the commands for those actuators are reduced proportionally to the limit. We know this is working in our code since the limits occasionally engage when gains are too high causing the loop to diverge or a poorly constructed basis set is used.

We also monitor the overall peak-to-valley stroke of the BMC and Alpao mirrors in our simulations. The BMC is typically less than 1 μm P2V, and the Alpao is typically less than 3 μm P2V. These are well within the limits of the chosen DMs as well.

The key conclusion we have reached from our simulations is that the inter-actuator strokes of the devices are sufficient for Kolmogorov turbulence at LCO. We have already procured an Alpao DM97-15 which will allow us to develop a suitable slaving model for its un-illuminated actuators and validate our model of it.

3.3 Basis Sets: When simulating the MagAO-as-1st-stage option, the MagAO system is simulated using the KL basis used on sky. For MagAO-X we construct a basis set from a 40x40 square grid of Fourier modes which is augmented with the first 10 Zernike polynomials.

The basis set for MagAO-X with a woofer is constructed in the following steps:

- A custom KL basis is constructed as a decomposition of a 10x10 grid of Fourier modes for the von Karman spectrum with tip and tilt subtracted. Using the Fourier basis instead of the usual Zernike polynomials allows us to control the spatial frequency content of this basis and avoid the high derivatives at the edge of the pupil that occur with the Zernikes. We keep the first 48 modes of this basis.
- the KL basis is then augmented with pure tip and tilt modes. This forms a 50-mode low-order basis used for the woofer.
- For the tweeter, we use an NxN grid of Fourier modes, where the N used depends on star brightness. N ranges from 22 to 42 depending on star brightness.

So far we do not explicitly orthogonalize the woofer-tweeter bases. Rather, we depend on the SVD in the reconstructor pseudo-inverse to find an orthogonal projection. In simulations this works and we have stable loops. We recognize that this may not be optimal, and we are investigating various orthogonalization strategies as well.

3.4 Control Law: For MagAO we calculate slopes from the CCD-39 simulated detector and use a pure-integrator control law as is standard. MagAO loop parameters (speed, gains, WFS binning) were adjusted to optimize the performance of MagAO-X. A key point is that the control-loop dynamics of these cascaded loops were fully simulated.

For MagAO-X we calculate slopes from the OCAM-2K simulated images. Here we use a leaky integrator control law and find that it performs better than the pure integrator. Modal gains were optimized using PSDs (Smith & Véran, 2003; Poyneer & Véran, 2005) for various star magnitudes. When the woofer-tweeter system is simulated, the Alpao woofer is given a longer settling time (0.5 ms) than the BMC (0.25 ms, minimum time-step in simulation). This simulates the different dynamics of the two devices.

3.5 Turbulence Simulation: We used a model of the LCO atmosphere based on the GMT site survey Prieto et al. (2010) and LCO seeing statistics and outer scale $L_0 = 25$ mFloyd et al. (2010). We use only DIMM seeing to have a valid measure of r_0 independent of L_0. In our end-to-end simulations we include the outer scale (von Kármán statistics) and the median C_n^2 profile. We simulated multiple layers using the C_n^2 profile from site testingPrieto et al. (2010), propagating with characteristic wind velocities.

We normally have little knowledge of wind speed at altitude. We incorporate our own experience at LCO (*many* nights on-sky with MagAO) to estimate typical winds. As a baseline we use the GMT survey wind layers, which have a C_n^2 weighted mean of $\bar{v} = 18.7$ m/s. To model good conditions, we use winds 50% slower.

We summarize our atmosphere model in Table 5. For this analysis we use 2 distinct models, intended to represent "excellent", and "good" conditions. The "25%" model corresponds to first quartile DIMM seeing, and low winds. The "50%" model corresponds to median DIMM seeing, and the GMT atmosphere winds. We also show our "75%" model, which includes third quartile DIMM seeing, and higher winds. Wind and seeing are not necessarily coupled, so various combinations of these parameters are possible.

Table 5: Summary of MagAO Atmosphere Models

Quartile	$\bar{v}$	@ V (0.5 μm)		
		FWHM	r_0	τ_0
	[m/s]	["]	[m]	[msec]
25%	9.4	0.51	0.20	7.4
50%	18.7	0.65	0.16	2.9
75%	23.4	0.81	0.13	1.9

4 Results

Simulations were run over a range of guide star magnitudes for median and 25%-ile conditions. The Strehl ratio results are shown in Figure 7 for the typical MEMS surface quality, and Figure 8 for the worst case MEMS surface quality. See Section 5.1 for the static and NCP error budget.

Next we show unocculted PSFs as well as coronagraphic PSFs using the vAPP (design described in 5.2 below) for 30 second exposures. We also show contrast profiles through the dark hole. In the contrast profile plots, photon noise limits are shown which take into account the Strehl both due to AO performance and the vAPP Strehl, as

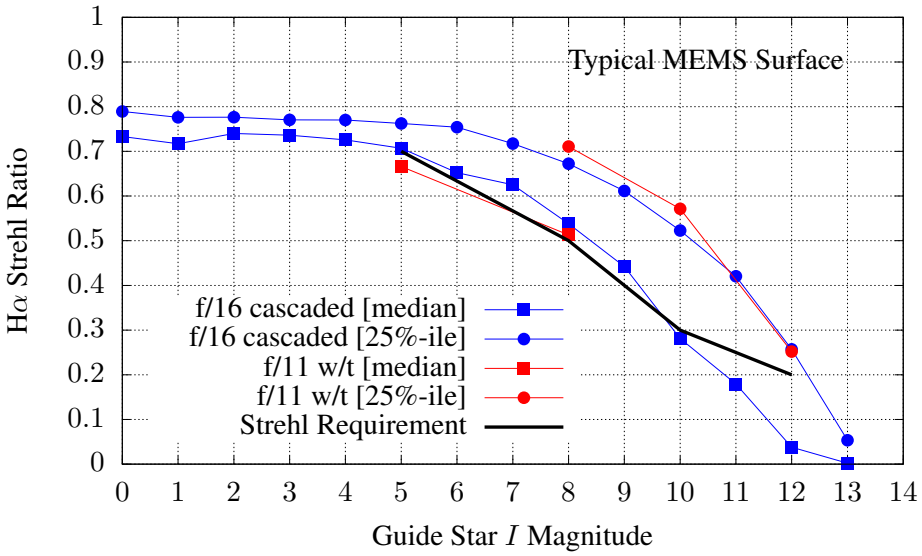

Figure 7: Strehl vs guide magnitude from simulations. The static and NCP error budget from Section 5.1 is include for the typical MEMS surface quality. The Strehl requirement is met for 25%-ile conditions. We are close to the Strehl goal for stars brighter than I=10mag, meaning that median conditions can be used for MaXProtoPlanets.

well as the typical MEMS case static and NCP. The photon noise is calculated for the custom designed Hα filter presented in 2.1, with throughputs a shown in 5.4 below.

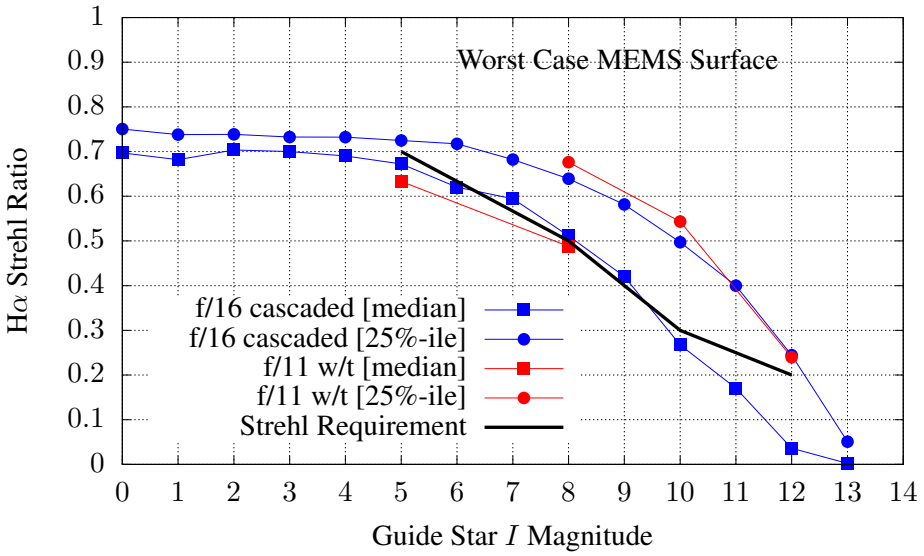

Figure 8: Strehl vs guide magnitude from simulations. The static and NCP error budget from Section 5.1 is include for the worst case MEMS surface quality. The Strehl requirement is met for 25%-ile conditions. For bright stars, we are limited by static and NCP dominated by the worst case DM. We are still close enough to the Strehl goal for stars brighter than I=10mag, that we expect median conditions can be used for MaXProtoPlanets here as well.

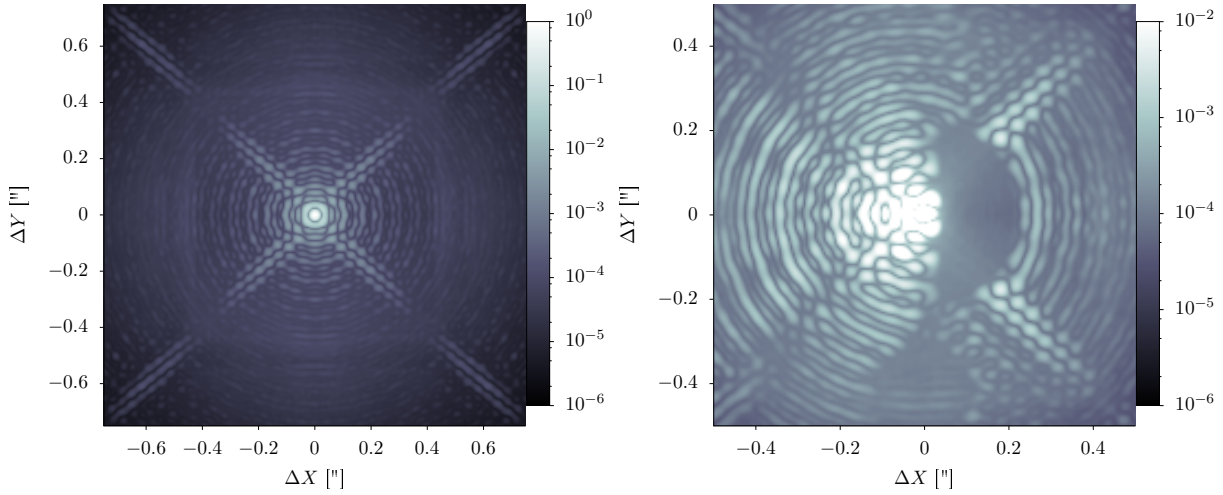

Figure 9: PSF for an 8th magnitude star in 25%-ile conditions.

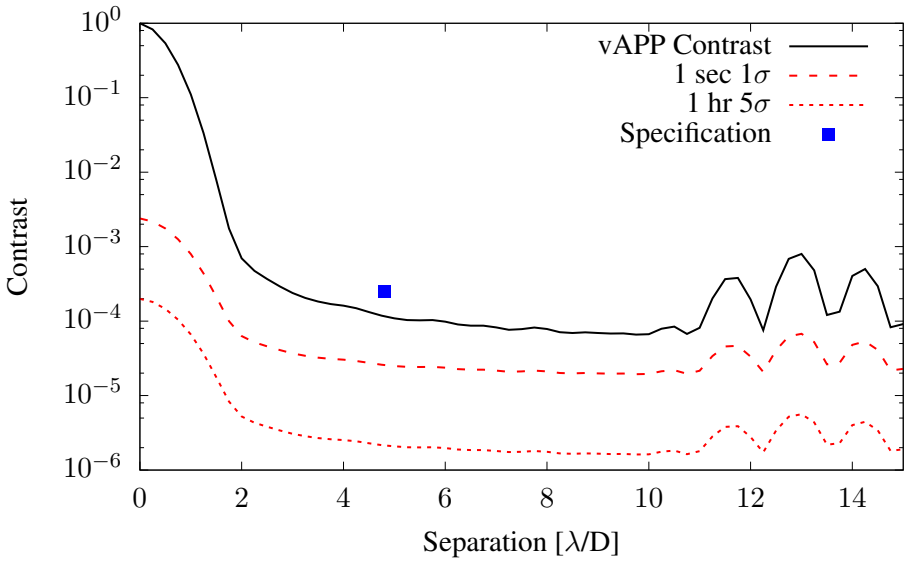

Figure 10: Contrast for an 8th magnitude star in 25%-ile conditions. The contrast at 100 mas (5 λ/D) meets the specification of 2.5×10^{-4}.

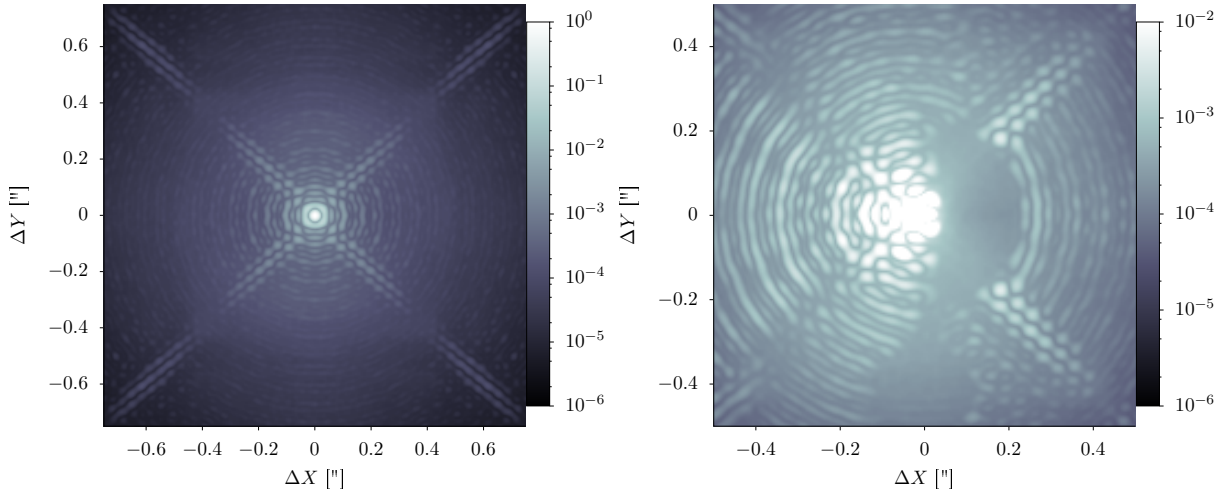

Figure 11: PSF for a 10th magnitude star in 25%-ile conditions.

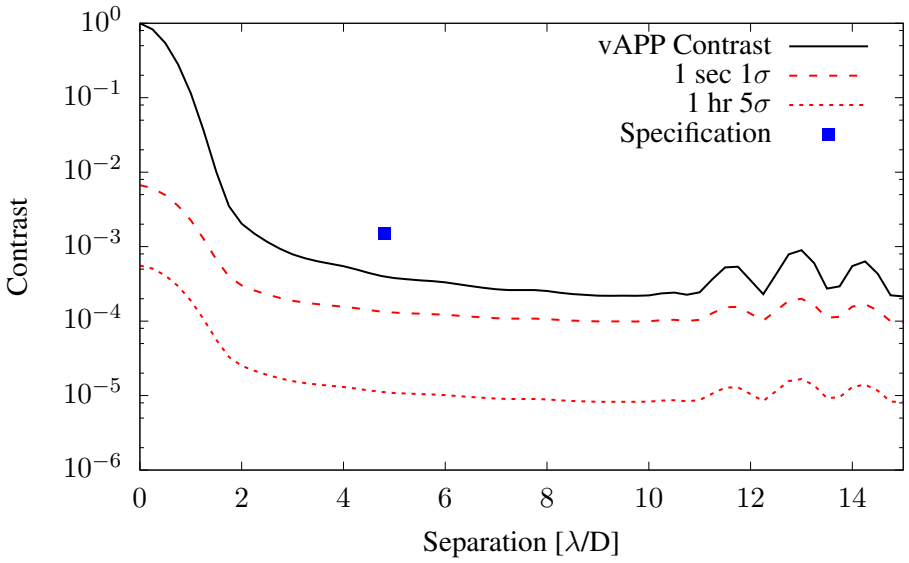

Figure 12: Contrast for a 10th magnitude star in 25%-ile conditions. The contrast at 100 mas (5 λ/D) meets the specification of 1.5×10^{-3}

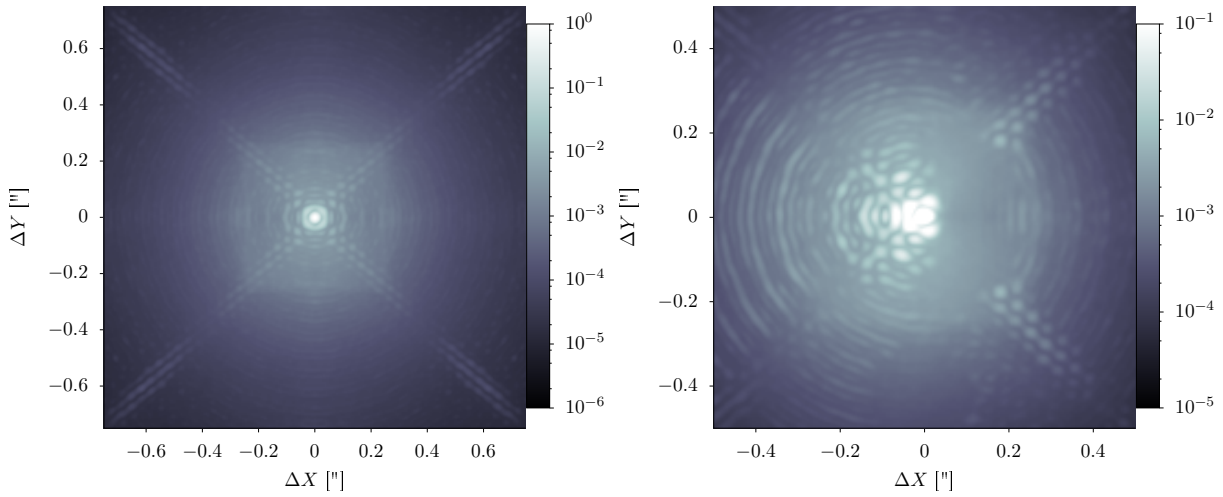

Figure 13: PSF for a 12th magnitude star in 25%-ile conditions.

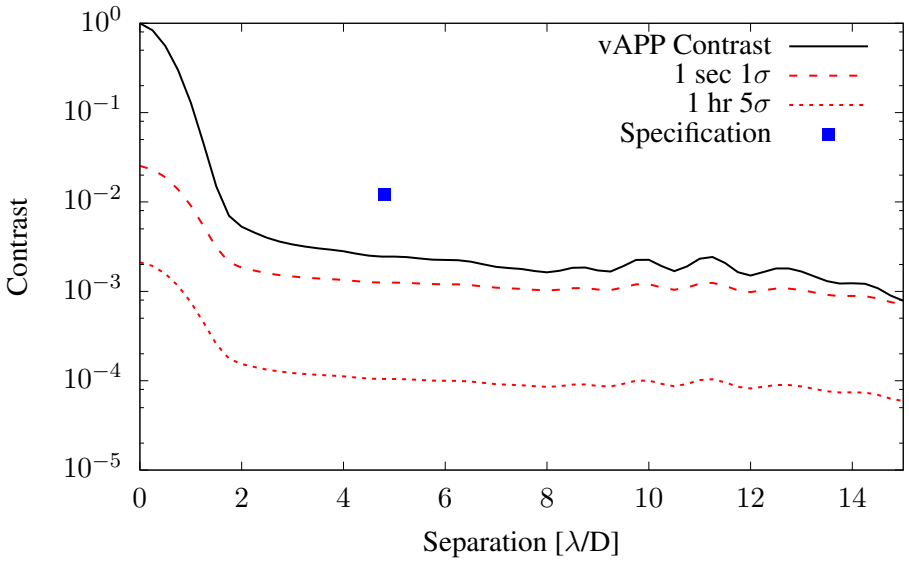

Figure 14: Contrast for an 12th magnitude star in 25%-ile conditions. The contrast at 100 mas (5 λ/D) meets the specification of 1.0×10^{-2}

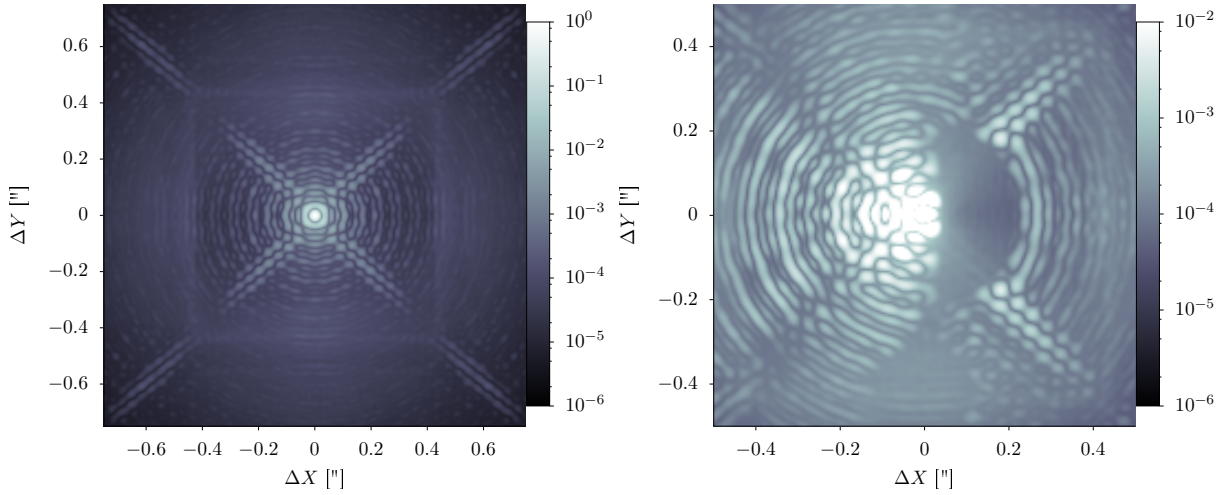

Figure 15: PSF for a 5th magnitude star in 50%-ile conditions.

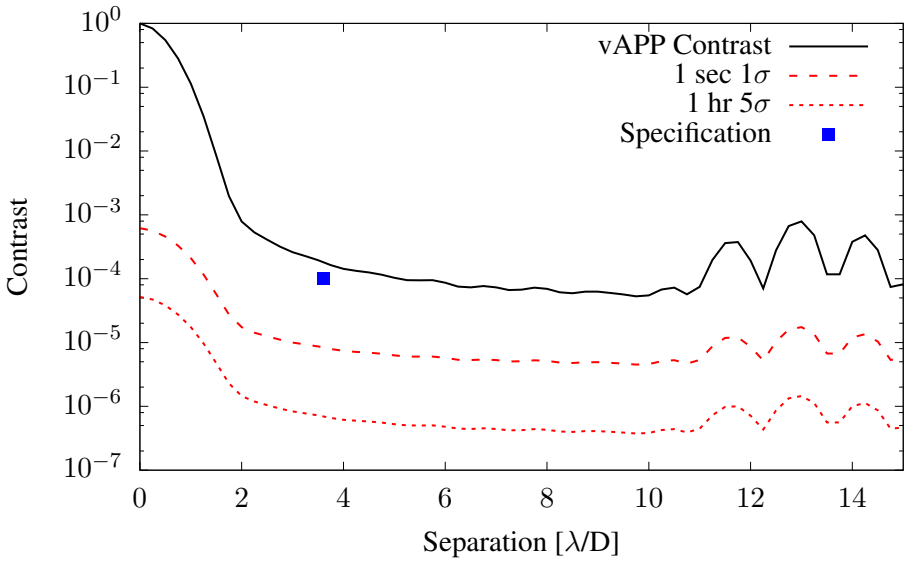

Figure 16: Contrast for a 5th magnitude star in 50%-ile conditions. This is our most demanding requirement. The raw contrast at 75 mas (3.5 λ/D) is below the specification, however the photon noise limits are well below. This means that we will be able to sense (using LOWFS and FPWFS) and calibrate (using SDI) the residuals to meet the detection requirement of 1.0×10^{-4} even in median conditions.

5 Conclusion

End-to-end simulations have shown that the MagAO-X design can deliver the wavefront quality needed for MaXProtoPlanets. Strehl ratio (a soft requirement), is met in 25%-ile conditions with margin, and we reach or come close to the goal of working in median conditions. Most importantly, we meet the contrast requirements. The raw turbulence limited contrast, as well as the photon noise from the residual, is below the spec in 25% conditions. Even in median conditions, the 5th mag star case shows that we can meet our most demanding specification with SDI and LOWFS and FPWFS techniques.

References

Floyd, D. J. E., Thomas-Osip, J., & Prieto, G. 2010, PASP, 122, 731

Poyneer, L. A., & Véran, J.-P. 2005, Journal of the Optical Society of America A, 22, 1515

Prieto, G., Thomas-Osip, J. E., Phillips, M. M., McCarthy, P., & Johns, M. 2010, Proc. SPIE, 7733, 773340

Smith, M. J., & Véran, J.-P. 2003, Proc. SPIE, 4839, 964